A Trans-Spanning Diphosphine Ligand Based on a *m*-Terphenyl Scaffold and Its Palladium and Nickel Complexes

Rhett C. Smith and John D. Protasiewicz*

Department of Chemistry, Case Western Reserve University, Cleveland, Ohio 44106-7708

Received May 13, 2004

The new diphosphine ligand 2,6-bis(2-((diphenylphosphino)methyl)phenyl)benzene (**1**) has been prepared for potential use as a terdentate pincer-type ligand. Upon examination of the coordination chemistry with representative palladium and nickel centers, however, it was discovered that it acts as a bidentate trans-spanning ligand upon coordination to form *trans*-[(**1**)$PdCl_2$] (**2**) and *trans*-[(**1**)$NiCl_2$] (**3**). Attempts to promote CH activation of the central benzene ring and produce a terdentate pincer binding mode for **1** were unsuccessful. Reaction of **2** and $[Li(OEt_2)][B(C_6F_5)_4]$ led to formation of the dicationic bis(chloro)-bridged dimer $[(\mathbf{1})_2\{Pd_2(\mu_2\text{-}Cl)_2\}][B(C_6F_5)_4]_2$ (**4**), in which two ligands **1** have rearranged to span across the dichlorodipalladium core. The structures of air- and moisture-stable **2**−**4** were confirmed by X-ray crystallography.

Introduction

The utility of phosphines as ligands in metal complexes, and particularly the effect of phosphine selection on catalysis, has made the synthesis and investigation of novel phosphines an area of ongoing interest. Some key phosphine properties to be considered are cone angle,[1] bite angle,[2] and basicity.[3] For example, structural and catalytic effects of unusually bulky phosphines are a topic of current investigation.[4] There have also been a number of studies on wide bite angle[2] and trans-spanning bidentate phosphines[5] which have demonstrated advantageous effects on a number of catalytic processes.[2,5,6] Simple *m*-xylyl-anchored terdentate "pincer" ligands (Scheme 1; **A**, D = various donors such as PR_2, NR_2, etc.) have attracted particular interest.[7] One advantage of such systems is that the preparation of ligands featuring a variety of donor elements is readily accomplished by starting from α,α′-dibromo-*m*-xylene (Scheme 1, top left). Metal complexes featuring pincer ligands have been employed in a number of studies such as C−C, C−H, C−N, and C−Si bond activation, as gas sensors, and as molecular switches. Catalytic applications studied include Heck and Suzuki coupling reactions, hydrogen transfer, dehydrogenation, hydroamination, and polymerizations.[7]

Although pincer ligands have been fruitfully employed and exhibit rigid terdentate binding modes, such ligands often lack an inherent three-dimensional ligand backbone that may be desirable for tuning catalytic processes. The *m*-terphenyl scaffold has been used to access a variety of interesting molecular geometries and coordination environments.[8] Recently Rabe has reported the first pincer type ligands having a *m*-terphenyl backbone (**B** with D = OMe; Scheme 1) and their application in the preparation of lanthanide complexes.[9] As opposed to following the process(es) outlined in Scheme 1 that

(1) (a) Tolman, C. *Chem. Rev.* **1977**, *77*, 313−348. (b) Caffery, M. L.; Brown, T. L. *Inorg. Chem.* **1991**, *30*, 3907−3914. (c) Lee, K. J.; Brown, T. L. *Inorg. Chem.* **1992**, *31*, 289−294. (d) Brown, T. L. *Inorg. Chem.* **1992**, *31*, 1286−1294.

(2) (a) van der Veen, L. A.; Boele, M. D. K.; Bergman, F. R.; Kamer, P. C. J.; van Leeuwen, P. W. N. M.; Goubitz, K.; Fraanje, J.; Schenk, H.; Bo, C. *J. Am. Chem. Soc.* **1998**, *120*, 11616−11626. (b) Kamer, P. C. J.; van Leeuwen, P. W. N. M.; Reek, J. N. H. *Acc. Chem. Res.* **2001**, *34*, 895−904. (c) van Leeuwen, P. W. N. M.; Kamer, P. C. J.; Reek, J. N. H.; Dierkes, P. *Chem. Rev.* **2000**, *100*, 2741−2769.

(3) (a) Joerg, S.; Drago, R. S.; Sales, J. *Organometallics* **1998**, *17*, 589−599. (b) Drago, R. S.; Joerg, S. *J. Am. Chem. Soc.* **1996**, *118*, 2654−2663. (c) Drago, R. S. *Organometallics* **1995**, *14*, 3408−3417. (d) Sowa, J. R.; Zanotti, V.; Angelici, R. J. *Inorg. Chem.* **1993**, *32*, 848−853. (e) Sowa, J. R.; Zanotti, V.; Facchin, G.; Angelici, R. J. *J. Am. Chem. Soc.* **1991**, *113*, 9185−9192. (f) Sowa, J. R.; Angelici, R. J. *Inorg. Chem.* **1991**, *30*, 3534−3537. (g) Bodner, G. M.; May, M. P.; McKinney, L. E. *Inorg. Chem.* **1980**, *19*, 1951−1958. (h) Pacchioni, G.; Bagus, P. S. *Inorg. Chem.* **1992**, *31*, 4391−4398.

(4) (a) Nagata, K.; Takeda, N.; Tokitoh, N. *Chem. Lett.* **2003**, *32*, 170−171. (b) Nagata, K.; Takeda, N.; Tokitoh, N. *Phosphorus Sulfur Relat. Elem.* **2002**, *177*, 1859−1862. (c) Chen H.-P.; Liu, Y.-H.; Peng, S.-M.; Liu, S.-T. *Dalton* **2003**, 1419−1424. (d) Bell, N. A.; Coles, S. J.; Constable, C. P.; Hursthouse, M. B.; Light, M. E.; Mansor, R.; Salvin, N. J. *Polyhedron* **2002**, *21*, 1845−1855. (e) Albert, J.; Bosque, R.; Cadena, J. M.; Delgado, S.; Granell, J.; Muller, G.; Ordinas, J. I.; Bardia, M. F.; Solans, X. *Chem. Eur. J.* **2002**, *8*, 2279−2287. (f) Xu, X.; Nieuwenhuyzen, M.; James, S. L. *Angew. Chem., Int. Ed.* **2002**, *41*, 764−767. (g) Matsumoto, T.; Kasai, T.; Tatsumi, K. *Chem. Lett.* **2002**, *3*, 346−347. (h) Stuer, W.; Wolf, J.; Werner, H. *J. Organomet. Chem.* **2002**, *641*, 203−207. (i) Alyea, E. C.; Ferguson, G.; Kannan, S. *Polyhedron* **2000**, *19*, 2211−2213. (j) Bell, N. A.; Coles, S. J.; Hursthouse, M. B.; Light, M. E.; Malik, K. A.; Mansor, R. *Polyhedron* **2000**, *19*, 1719−1726. (k) Yamamoto, Y.; Kawasaki, K.; Nishimura, S. *J. Organomet. Chem.* **1999**, *587*, 49−57. (l) Reid, S. M.; Boyle, R. C.; Mague, J. T.; Fink, M. J. *J. Am. Chem. Soc.* **2003**, *125*, 7816−7817. (m) Shenglof, M.; Gelman, D.; Heymer, B.; Schumann, H.; Molander, G. A.; Blum, J. *Synthesis* **2003**, *2*, 302−306. (n) Li, G. Y. *J. Org. Chem.* **2002**, *67*, 3643−3650. (o) Lee, S.; Jorgensen, M.; Hartwig, J. F. *Org. Lett.* **2001**, *3*, 2729−2732. (p) Liu, S.-Y.; Choi, M. J.; Fu, G. C. *Chem. Commun.* **2001**, 2408−2409. (q) Dai, C.; Fu, G. C. *J. Am. Chem. Soc.* **2001**, *123*, 2719−2724. (r) Littke, A. F.; Dai, C.; Fu, G. C. *J. Am. Chem. Soc.* **2000**, *122*, 4020−4028. (s) Remmele, H.; Koellhofer, A.; Plenio, H. *Organometallics* **2003**, *22*, 4098−4103. (t) Kollhofer, A.; Plenio, H. *Chem. Eur. J.* **2003**, *9*, 1416−1425. (u) Ehrentraut, A.; Zapf, A.; Beller, M. *Adv. Synth. Catal.* **2002**, *344*, 209−217. (v) Stauffer, S. R.; Beare, N. A.; Stambuli, J. P.; Hartwig, J. F. *J. Am. Chem. Soc.* **2001**, *123*, 4641−4642. (w) Stambuli, J. P.; Stauffer, S. R.; Shaughnessy, K. H.; Hartwig, J. F. *J. Am. Chem. Soc.* **2001**, *123*, 2677−2678. (x) Zapf, A.; Ehrentraut, A.; Beller, M. *Angew. Chem., Int. Ed.* **2000**, *39*, 4153−4155. (y) Reid, S. M.; Boyle, R. C.; Mague, J. T.; Fink, M. J. *J. Am. Chem. Soc.* **2003**, *125*, 7816−7817. (z) Matsumoto, T.; Kasai, T.; Tatsumi, K. *Chem. Lett.* **2002**, 346−346.

10.1021/om049662d CCC: $27.50
Publication on Web 07/29/2004

Scheme 1. Preparation and Reactivity of (Left) Pincer Ligands and (Right) Possible Parallel Transformations with Terphenyl-Based Ligands[a]

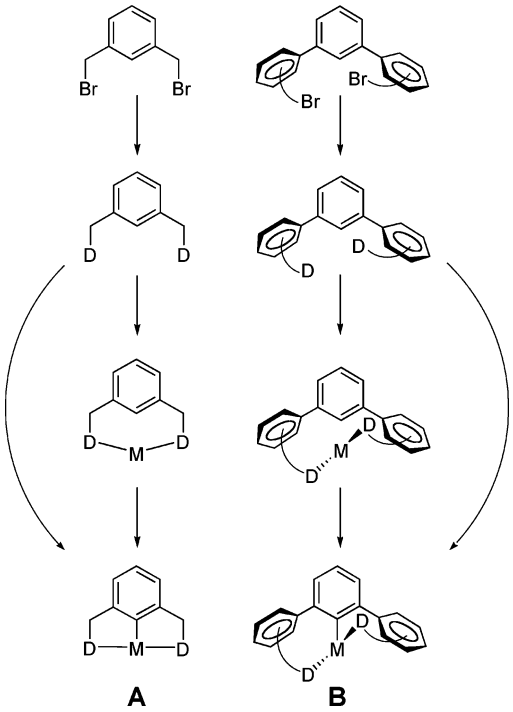

[a] D = various donor groups such as NR_2, PR_2, OR, etc.

involve activation of the CH bond of a benzene ring, successful entry into these complexes was affected by use of the lithium salt of the 2,6-(*o*-anisyl)$_2$C$_6$H$_3$ ligand.

The simple synthetic methodology[10] for the preparation of *m*-terphenyls affords an opportunity for their development as attractive scaffolds upon which to build ligand frameworks. Specifically, by tethering metal-coordinating substituents to each of the flanking aryl rings (Scheme 1, right), ligands may be elaborated that exhibit properties similar to those of the *m*-xylyl-based pincer ligands but will have a more defined *three-dimensional* backbone and a possibly C_2-symmetric (chiral) geometry. Herein is reported the synthesis of a *m*-terphenyl-anchored diphosphine ligand and its use in preparing new Ni and Pd chloride complexes. Structural characterizations of three of these complexes reveal a surprising flexibility in the ligand binding mode.

Experimental Section

All manipulations were carried out in a drybox under an atmosphere of N_2. Anhydrous dichloromethane was purchased from Acros and used as received. Acetonitrile was distilled from CaH_2 under nitrogen; all other solvents were distilled from sodium benzophenone ketyl prior to use. Literature routes were used to prepare 2,2″-dimethyl-*m*-terphenyl,[11a] 2,2″-bis(bromomethyl)-*m*-terphenyl,[11c] and $PdCl_2(NCPh)_2$.[11f] $[Li(OEt_2)_{2.5}][B(C_6F_5)_4]$ was purchased from Boulder Scientific. NMR spectra were recorded on a Varian Gemini instrument operating at 300 MHz for proton measurements and 121.5 MHz for phosphorus. Proton and phosphorus spectra are referenced to residual solvent signals or 85% phosphoric acid, respectively. Variable-temperature ^{31}P NMR spectra were recorded in CD_2Cl_2 between −80 and +55 °C at a field strength of 121.5 MHz. Variable-temperature ^{1}H NMR spectra were recorded in $CDCl_3$ between −45 and +55 °C on a Varian Inova 600 MHz NMR instrument.

2,6-{2-(Ph$_2$PCH$_2$)C$_6$H$_4$}$_2$C$_6$H$_3$ (1). To a solution of diphenylchlorophosphine (3.05 g, 13.8 mmol) in THF (30 mL) was added freshly cut Li metal (0.200 g, 31.2 mmol). The resultant solution was stirred for 4 h at room temperature, over which time the mixture became warm, lithium was consumed, and a red color developed. The resultant red solution was decanted from the excess Li pieces and cooled to −78 °C. To the chilled solution was added a solution of 2,2″-bis(bromomethyl)-*m*-terphenyl (2.50 g, 6.01 mmol) in THF (30 mL) via cannula. The resultant solution was warmed to room temperature and stirred for an additional 6 h. All volatiles were removed in vacuo, and the residue was taken up in 40 mL of diethyl ether. This solution was washed with two 10 mL aliquots of water and then dried over Na_2SO_4. Removal of volatiles under reduced pressure produced a white powder. Final purification was affected by recrystallization from a saturated CH_2Cl_2 solution at −35 °C to give **1** as white needlelike crystals (2.82 g, 60.3%). ^{1}H NMR ($CDCl_3$): δ 3.44 (s, 4H), 7.05−7.24 (m, 31H), 7.31 (t, 1H, J = 7 Hz). ^{31}P NMR ($CDCl_3$): δ −8.8. Mp: 148−151 °C.

[(1)PdCl$_2$] (2). A solution of **1** (0.279 g, 0.449 mmol) and $PdCl_2(NCPh)_2$ (0.144 g, 0.449 mmol) in CH_2Cl_2 (30 mL) was stirred at room temperature for 10 min. All volatiles were removed under reduced pressure. The solid was rinsed with *n*-pentane, and then diethyl ether, to afford **2** as a yellow powder (0.349 g, 97.2%). Analytically pure crystalline **2** was obtained by diffusion of tetramethylsilane into a saturated dichloromethane solution. ^{1}H NMR (C_6D_6): δ 3.06 (d, 2H, J = 12 Hz), 4.80 (d, 2H, J = 12 Hz), 5.96 (d, 2H, J = 8 Hz), 6.68 (t, 1H, J = 8 Hz), 7.10−7.31 (m, 28H), 8.02 (s, 1H). ^{31}P NMR ($CDCl_3$): δ 16.1. Anal. Calcd for $C_{44}H_{36}Cl_2P_2Pd$: C, 65.73; H, 4.51. Found: C, 65.58; H, 4.36.

[(1)NiCl$_2$] (3). A solution of **1** (0.071 g, 0.11 mmol) and $NiCl_2(DME)$[12] (0.025 g, 0.11 mmol) in CH_2Cl_2 (3 mL) was allowed to stand at room temperature for 8 h, over which time

(5) (a) Bessel, C. A.; Aggarwal, P.; Marchilok, A. C.; Takeuchi, K. J. *Chem. Rev.* **2001**, *101*, 1031−1066. (b) Yin, J.; Buchwald, S. L. *J. Am. Chem. Soc.* **2002**, *124*, 6043−6048. (c) Freixa, Z.; van Leeuwen, P. W. N. M. *Dalton* **2003**, 1890−1901. (d) Alcock, N. W.; Brown, J. M.; Jeffery, J. C. *J. Chem. Soc., Chem. Commun.* **1974**, 829−830. (e) March, F. C.; Mason, R.; Thomas, K. M.; Shaw, B. L. *J. Chem. Soc., Chem. Commun.* **1975**, 584−585. (f) March, F. C.; Mason, R.; Thomas, K. M.; Shaw, B. L. *J. Chem. Soc., Chem. Commun.* **1975**, 584. (g) Bachechi, F.; Zambonelli, L.; Venanzi, L. M. *Helv. Chim. Acta* **1977**, *60*, 2815−2823. (h) Bachechi, F.; Zambonelli, L.; Venanzi, L. M. *Helv. Chim. Acta* **1977**, *60*, 2815−2823. (i) Kamer, P. C. J.; van Leeuwen, P. W. N. M.; Reek, J. N. H. *Acc. Chem. Res.* **2001**, *34*, 895−904.

(6) (a) Shaw, B.; Perera, S. D. *Chem. Commun.* **1998**, 1863−1864. (b) van der Veen, L. A.; Kamer, P. C. J.; van Leeuwen, P. W. N. M. *Angew. Chem., Int. Ed.* **1999**, *38*, 336−338. (c) van der Veen, L. A.; Keeven, P. K.; Kamer, P. C. J.; van Leeuwen, P. W. N. M. *Dalton* **2000**, 2105−2112.

(7) (a) Albrecht, M.; van Koten, G. *Angew. Chem., Int. Ed.* **2001**, *40*, 3750−3781. (b) van der Boom, M. E.; Milstein, D. *Chem. Rev.* **2003**, *103*, 1759−1792.

(8) (a) Twamley, B.; Haubrich, S. T.; Power, P. *Adv. Organomet. Chem.* **1999**, 1−65. (b) Clyburne, J. A. C.; McMullen, N. *Coord. Chem. Rev.* **2000**, *210*, 73−99. (c) Robinson, G. H. *Acc. Chem. Res.* **1999**, *32*, 773. (d) Hart, H. *Pure Appl. Chem.* **1993**, *65*, 27−34.

(9) (a) Rabe, G.; Zhang-Presse, M.; Riederer, F. A.; Yap, G. P. A. *Inorg. Chem.* **2003**, *42*, 3527−3533. (b) Rabe, G. W.; Zhang-Presse, M.; Golen, J. A.; Rheingold, A. L. *Acta Crystallogr., Sect. E* **2003**, *E59*, m1102−m1103. (c) Rabe, G. W.; Zhang-Presse, M.; Riederer, F. A.; Golen, J. A.; Incarvito, C. D.; Rheingold, A. L. *Inorg. Chem.* **2003**, *42*, 7587−7592. (d) Rabe, G. W.; Rhatigan, B.; Golen, J. A.; Rheingold, A. L. *Acta Crystallogr., Sect. E* **2003**, *E59*, m99−m101. (e) Rabe, G. W.; Zhang-Presse, M.; Yap, G. P. A. *Acta Crystallogr., Sect. E* **2002**, *E58*, m434−m435. (f) Rabe, G. W.; Berube, C. D.; Yap, G. P. A. *Inorg. Chem.* **2001**, *40*, 4780−4784.

(10) Saednya, A.; Hart, H. *Synthesis* **1996**, 1455−1458.

(11) (a) Vinod, T. K.; Hart, H. *J. Org. Chem.* **1990**, *55*, 5461−5466. (b) Voegtle, F.; Schunder, L. *Justus Liebigs Ann. Chem.* **1969,** *721*, 129−132. (c) Hammerschmidt, E.; Bieber, W.; Voegtle, F. *Chem. Ber.* **1978,** *111*, 2445−2447. (d) Josel, H. P.; Loehr, H. G.; Engel, A.; Rapp, J.; Voegtle, F.; Franken, S.; Puff, H., *J. Incl. Phenom.* **1985,** *3*, 43−50. (e) Chiu, J. J.; Grewal, R. S.; Hart, H.; Ward, D. L. *J. Org. Chem.* **1993,** *58*, 1553−1559. (f) Kharasch, M. S.; Seyler, R. C.; Mayo, F. R. *J. Am. Chem. Soc.* **1938**, *60*, 882−884.

Table 1. Crystal Data and Structure Refinement Details for 2−4

	2	3	4
empirical formula	$C_{44}H_{36}Cl_2P_2Pd$	$C_{44}H_{36}Cl_2NiP_2$	$C_{146}H_{96}B_2Cl_2F_{40}P_4Pd_2$
fw	803.97	756.28	3039.43
temp (K)	298	298	298
wavelength (Å)	0.710 73	0.710 73	0.710 73
cryst syst	monoclinic	monoclinic	triclinic
space group	$P2_1/n$	$P2_1/n$	$P\bar{1}$
unit cell dimens			
a (Å)	13.123(2)	12.9651(18)	14.379(3)
b (Å)	10.3739(18)	10.3559(15)	15.2099(19)
c (Å)	27.945(8)	28.028(5)	16.078(2)
α (deg)	90.00	90.00	88.431(12)
β (deg)	101.182(12)	101.978(14)	82.665(15)
γ (deg)	90.00	90.00	82.108(17)
V (A^3)	3732.2(14)	3681.2(10)	3454.3(10)
Z	4	4	1
calcd density (Mg/m^3)	1.431	1.365	1.461
abs coeff (mm^{-1})	0.757	0.790	0.450
F(000)	1640	1568	1528
cryst size (mm)	0.30 × 0.24 × 0.12	0.34 × 0.24 × 0.16	0.28 × 0.14 × 0.10
cryst color and shape	yellow plate	violet block	yellow block
θ range, data collecn (deg)	2.74−48.00	2.74−48.00	2.74−48.00
limiting indices	$-1 < h < 15$	$-1 < h < 14$	$-1 < h < 16$
	$-11 < k < 1$	$-1 < k < 11$	$-17 < k < 17$
	$-31 < l < 31$	$-32 < l < 31$	$-18 < l < 18$
no. of rflns collected	5848	5738	10 809
no. of indep rflns	3768	3735	5547
refinement method		full-matrix least squares on F^2	
no. of data/restraints/params	5848/0/437	5738/0/442	10809/0/858
goodness of fit on F^2	1.083	1.051	1.042
final R indices ($I > 2\sigma(I)$)[a,b]			
R1	0.0533	0.0469	0.0787
wR2	0.0917	0.0864	0.1873
R indices (all data)			
R1	0.1077	0.0979	0.1756
wR2	0.1115	0.1075	0.2327

[a] $R(F) = \sum||F_o| - |F_c||/\sum|F_o|$. [b] $R_w(F^2) = [\sum\{w(F_o^2 - F_c^2)^2\}/\sum\{w(F_o^2)^2\}]^{0.5}$; $w^{-1} = \sigma^2(F_o^2) + (aP)^2 + bP$, where $P = [F_o^2 + 2F_c^2]/3$ and a and b are constants adjusted by the program.

deep violet crystals formed. The crystals were collected by filtration and dried to afford 0.088 g of **3** (83%). ^{1}H NMR (CD_2Cl_2): δ 3.48 (virtual quartet, 4H, $^2J + {}^4J = 7$ Hz), 6.02 (d, 2H, $J = 8$ Hz), 6.77 (t, 1H, $J = 8$ Hz), 7.00−7.60 (m, 28H), 8.93 (s, 1H). ^{31}P NMR ($CDCl_3$): δ 4.9. Anal. Calcd for $C_{44}H_{36}Cl_2NiP_2$: C, 69.88; H, 4.80. Found: C, 69.71; H, 4.66.

[(1)$_2$Pd$_2$Cl$_2$][B(C$_6$F$_5$)$_4$]$_2$ (4). A solution of **2** (0.112 g, 0.140 mmol) and $[Li(OEt_2)_{2.5}][B(C_6F_5)_4]$ (0.122 g, 0.140 mmol) in CH_2Cl_2 was allowed to stand at room temperature for 24 h, over which time yellow crystals formed in the reaction vessel. Cooling the mixture to −35 °C caused further crystallization. The crystals were collected by filtration and dried in vacuo to afford **4** (0.157 g, 74.0%). ^{1}H NMR (CD_2Cl_2): δ 4.10 (m, 4H), 4.79 (m, 4H), 5.91 (d, 4H, $J = 8$ Hz), 6.47 (t, 2H, $J = 8$ Hz), 6.65, (s, 2H), 6.74−6.98 (m, 24H), 7.12−7.39 (m, 20H), 7.49−7.59 (m, 8H), 7.81−7.89 (m, 4H). ^{31}P NMR (CD_2Cl_2): δ 46.3. Anal. Calcd for $C_{136}H_{72}B_2Cl_2F_{40}P_4Pd_2$: C, 56.42; H, 2.51. Found: C, 55.74; H, 2.24.

X-ray Crystallography. Diffraction data were collected with a Siemens P4 instrument (Mo Kα radiation ($\lambda = 0.710\ 73$ Å)). Crystals were mounted onto glass fibers using epoxy. Crystals were judged to be acceptable on the basis of ω scans and rotation photography. A random search located reflections to generate the reduced primitive cell, and cell lengths were corroborated by axial photography. Additional reflections with 2θ values near 25° were appended to the reflection array and yielded the refined cell constants. Data were collected as presented in Table 1 and were corrected for absorption (empirical ψ scans). Computations were performed using SHELXTL version 6.1 (Bruker AXS). Further details may be found within the CIF files provided as Supporting Information.

(12) Nylander, L. R.; Pavkovic, S. F. *Inorg. Chem.* **1970**, *9*, 1959−1960.

Scheme 2. Preparation of 1

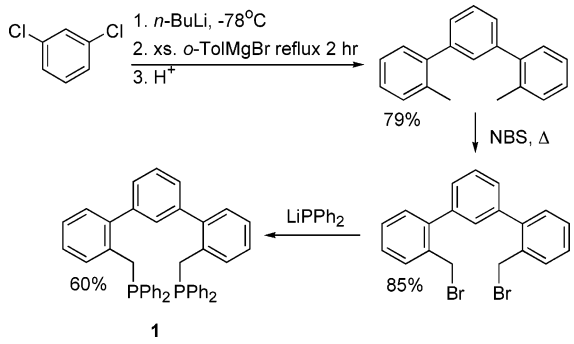

Results and Discussion

The synthesis of **1** was carried out in 40% yield over three steps, utilizing readily accessible starting materials (Scheme 2). The key precursor, 2,2″-bis(bromomethyl)-*m*-terphenyl,[11c] was chosen to allow for the future development of other new ligands featuring various donor elements upon reaction at the benzyl bromide functionalities, by analogy to the methods used to prepare previously reported *m*-xylyl-based pincer ligands. In the current example, transformation to diphosphine **1** was effected by reaction of the dibromide with lithium diphenylphosphide (Scheme 2). Ligand **1** displays a single ^{31}P NMR resonance at δ −8.8 ppm in $CDCl_3$.

Complexes of **1** with palladium and nickel were obtained upon mixing **1** with $PdCl_2(NCPh)_2$ and $NiCl_2$-

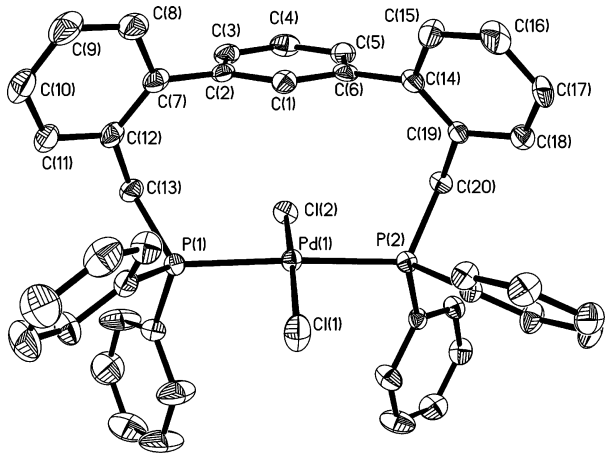

Figure 1. ORTEP drawing (30% probability ellipsoids) of the molecular structure of **2**. Hydrogen atoms are omitted for clarity.

Scheme 3. Preparation of 2 and 3

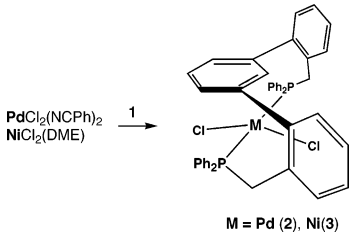

(DME) at room temperature in dichloromethane (Scheme 3). Analyses of these reaction mixtures by ^{31}P NMR spectroscopy revealed a single major product in each case with resonances at δ 16.1 and 4.9 ppm in $CDCl_3$ for the palladium and nickel complexes, respectively. Complexes **2** and **3** were readily isolated in 97 and 83% yields as pure materials that gave the correct analysis for the compositions of **1**·$PdCl_2$ and **1**·$NiCl_2$. ^1H NMR spectra of these materials were not definitive for complete structural assignments, owing to the presence of complex and broadened signals (vide infra).

Single crystals of each material were grown from diffusion of either tetramethylsilane (**2**) or *n*-pentane (**3**) into dichloromethane solutions of material at room temperature. The X-ray structural analysis of these compounds revealed coordination of **1** in a bidentate trans-spanning mode with P−M−P bite angles of 172.97(7)° in **2** and 174.77(5)° in **3** (Figure 1 shows a view of **2**). Crystals of **2** and **3** are isomorphous and thus have very similar structural parameters (Tables 1 and 2). The trans-spanning mode of **1** in these structures has some unusual structural consequences, as elucidated by the additional views of **2** shown in Figure 2. These representations highlight the facts that the central benzene ring lies roughly parallel to the $PdCl_2P_2$ plane and that H(1) (in its calculated position) and the palladium atom lie directly above one another at a distance of 3.48 Å (3.51 Å for the Ni complex). Additionally, one of the chlorine atoms (Cl(2)) lies directly below the center of the middle benzene ring of **1** at a relatively short distance of 3.33 Å. Short intramolecular M−Cl··· arene distances are not uncommon. A particularly striking example of the impact of a Pd−Cl···arene interaction is seen in the structure of [LPdCl][$PdCl_4$] (L = 6,6′-dimesityl-2,2′:6″,2″-terpyridine), where large distortions of the square-planar palladium center and

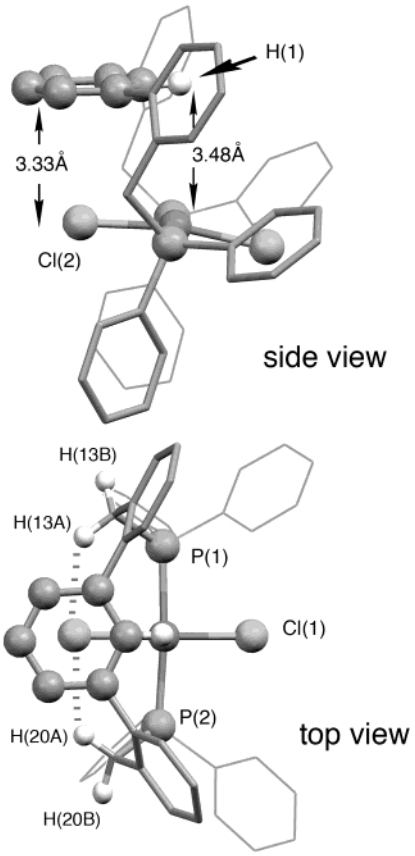

Figure 2. Further views of **2** emphasizing the conformation of **1**.

Table 2. Comparison of Select Bond Lengths (Å) and Angles (deg) for 2 (M = Pd) and 3 (M = Ni)

	2	3
M(1)−Cl(1)	2.2813(18)	2.1602(13)
M(1)−Cl(2)	2.3028(16)	2.1761(12)
M(1)−P(1)	2.3201(18)	2.2434(14)
M(1)−P(2)	2.3233(17)	2.2381(14)
Cl(1)−M(1)−Cl(2)	169.44(8)	166.42(6)
P(1)−M(1)−P(2)	172.97(7)	174.78(5)
Cl(1)−M(1)−P(1)	90.79(7)	92.11(5)
Cl(1)−M(1)−P(2)	92.68(7)	90.44(5)
Cl(2)−M(1)−P(1)	88.43(6)	87.72(5)
Cl(2)−M(1)−P(2)	87.05(6)	88.73(5)

a very short Cl···centroid distance of 3.29 Å are observed.[13] Despite the proximity of H(1) to the metal centers in **2** and **3**, clearly the metals have not inserted into this C−H bond. Two of the benzyl protons (H(13A) and H(20A)) are about 2.84 Å from Cl(2) (the hydrogen atoms being in their generated locations) in the X-ray structure of **2** (Figure 2; dashed lines indicate putative CH···Cl contacts). While this distance is somewhat outside the range for significant hydrogen-bonding interactions (see comparisons to **4**), the marked 1.74 ppm difference in chemical shifts for the protons that are directed inward toward Cl(2) (δ 4.80) and those that are directed outward (δ 3.06) suggest that in solution such interactions may be more significant. Alternatively, or in addition to these interactions, the location of these same protons under the central benzene ring may impart shifts due to ring anisotropy effects. Either

(13) Onoda, A.; Kawakita, K.; Okamura, T.-A.; Yamamoto, H.; Ueyama, N. *Acta* Crystallogr., Sect. E **2003**, *59*, m291−m293.

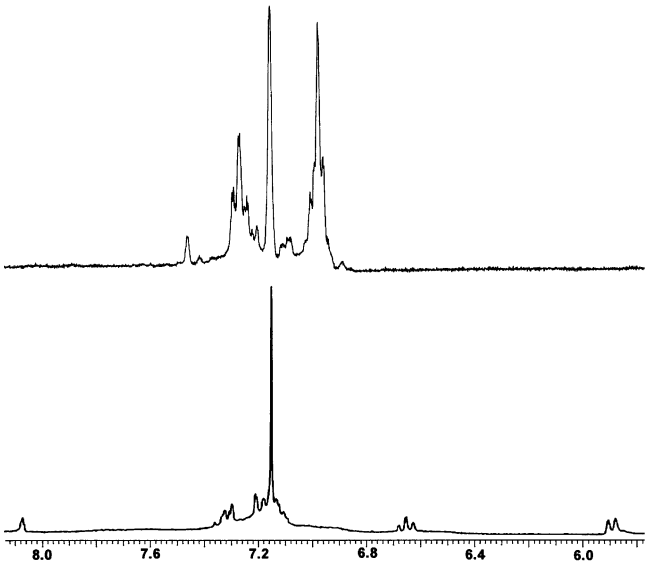

Figure 3. Comparison of partial ^{1}H NMR (300 MHz) spectra for the free ligand **1** (top) versus those of complex **2** (bottom) (recorded in C_6D_6; singlet resonances at 7.15 ppm correspond to residual C_6D_5H).

way, there are notable shift differences between the "inside" (A) and "outside" (B) protons on C(13) and C(20) of cyclic **2**.

Although **2** and **3** appear to display well-defined ligand environments in the solid state, analysis of their ^{1}H NMR spectra is not simple. These spectra display mixtures of broad and sharp signals, which are highly temperature and solvent dependent. While we do not have a comprehensive explanation of these spectra at this time, some details are notable and one possibility can be forwarded. These spectral features and their respective interpretations are thus presented in part to allow construction of a probable picture for the fluxionality of **2**.

First, Figure 3 illustrates that the ^{1}H NMR spectrum for **1** in C_6D_6 shows a large dispersion in chemical shifts upon its binding to the palladium center. These signals are attributed to the protons on the central benzene ring of **1**, due to its enforced proximity to the metal center. The proton that resides almost directly above the Pd atom (H(1)) resonates as a singlet at 8.02 ppm. The other protons for this ring resonate as a doublet at 5.96 ppm for H(3) and H(5) and a triplet at 6.68 ppm ($J = 8$ Hz) for H(4) and are easily assigned on the basis of the nature of the coupling patterns.

Second, all of the remaining aromatic signals are ill-defined, and some are broadened and lost into the baseline between 6.5 and 8 ppm. The nature of the spectra are solvent and temperature dependent. In solvents of increasing polarity ($C_6D_6 \ll CDCl_3 < CD_2Cl_2 \approx$ DMSO-d_6), additional, albeit broad, resonances are resolved. These observations may imply an interconversion that is rapid (on the ^{1}H NMR time scale) to another species that is more polar. Variable-temperature ^{31}P NMR spectra recorded between −80 and +55 °C in CD_2Cl_2 did not reveal any additional resonances or notable peak broadening/sharpening, making it unlikely that a major change in the phosphine coordination mode (from trans to cis, for example) is occurring. Proton NMR spectra were also obtained between −45 and +55 °C, in $CDCl_3$. These spectra revealed a marked sharpening of the broad resonances as the sample was cooled to −25 °C, with little change noted upon further cooling (Figures 4 and 5). No concentration dependence was noted for this behavior, ruling out bimolecular processes. The spectra shown in Figure 4 show that in $CDCl_3$ the "simple" picture for the central arene protons H(1) and H(4) is complicated by the resolution of additional minor signals. These signals, although fully resolved, suggest the presence of a minor isomer in solution that is in rapid equilibrium with a major form. In particular, a new signal near 8 ppm grows in as a doublet, suggesting that perhaps this might be attributable to the proton H(3) or H(5). If true, this result would indicate that the

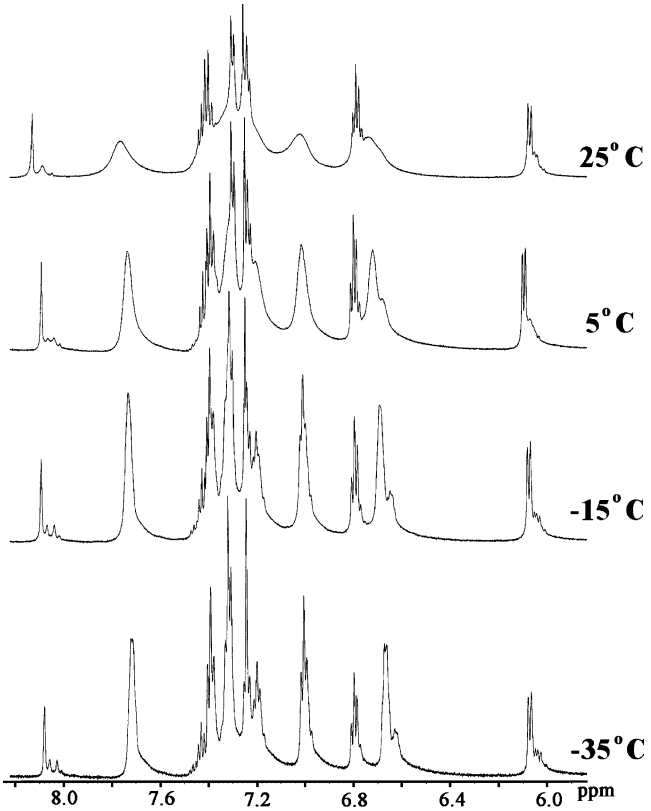

Figure 4. Temperature dependence of ^{1}H NMR (600 MHz, $CDCl_3$) signals for aromatic protons of **2**.

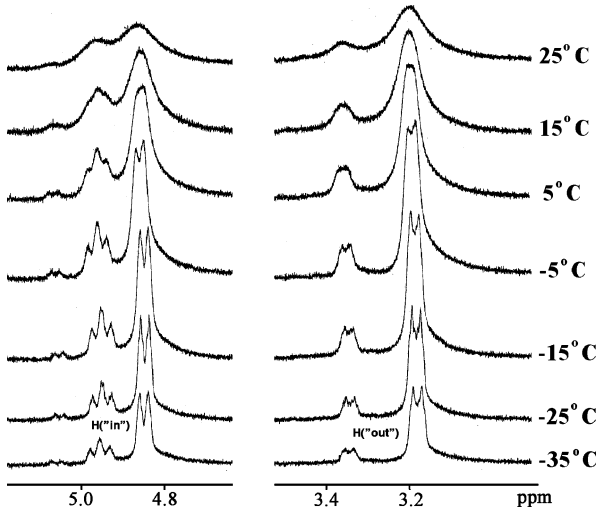

Figure 5. Temperature dependence of ^{1}H NMR (600 MHz, $CDCl_3$) signals for benzyl protons of **2**.

Scheme 4. Structures of Isomers of 2 and 2′[a]

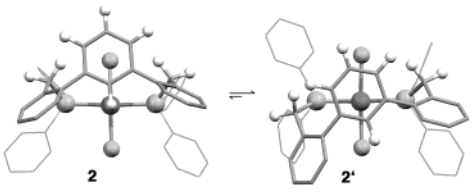

[a] Only key hydrogen atoms are shown for clarity.

position of the central benzene ring has moved in relationship to the $PdCl_2P_2$ "plane" and placed these protons in a position to feel the impact of the filled d_{z^2} orbital on palladium (or the presence of a chloride ligand) and, hence, have a downfield shift. Unfortunately, similar statements for the other protons of this ring are harder to claim, due to the lack of resolution and the fact that much of the spectrum in this area is dominated by the broad aromatic signals of the two other aromatic rings of the terphenyl group and the four other aromatic rings on the phosphorus atoms. Regardless, it appears that the fluxional process involves movement of nearly all protons of the ligand.

Third, and perhaps most revealing, is the variable-temperature behavior of the benzyl protons (Figure 5). While in C_6D_6 two signals are observed for H(13A)/H(20A) and H(13B)/H(20B), these signals appear as very broad signals in $CDCl_3$ at 300 MHz at room temperature. Examination of **2** by variable-temperature ^1H NMR spectroscopy at higher field (600 MHz) revealed the behavior shown in Figure 5. Cooling solutions of **2** to −35 °C allowed resolution of the broad signals into two sets of peaks. The relative ratio of the larger pair of signals to the smaller pair of signals is 3:1. As seen in C_6D_6, there is a ca. 1.5 ppm difference between two types of benzyl protons (the "inside" and "outside" protons). The more downfield resonances are again attributed to the "inside" benzyl protons. One of these signals, at 4.95 ppm, resolves into a triplet at low temperature (apparent J values for all four signals are 12−13 Hz), possibly indicating coupling to the $I = {}^1/_2$ ^{31}P nucleus or the presence of another isomer. These data suggest that two isomers are present and that each isomer has distinct environments for its "inside" and "outside" benzyl protons. At higher temperature (up to 55 °C) the signals get even broader and seem to disappear into the baseline. Such observations probably indicate that the exchange process involves H("in", major)/H("out" minor) and H("out", minor)/H("in" minor) pairs of signals, as increasing exchange between nearest neighboring signals would have led to some sharpening of the signals at higher temperatures.

Insights to this perplexing set of data were gained by semiempirical (SPARTAN '04, PM3) molecular modeling of **2**. Minimization of **2** starting with the X-ray structure coordinates resulted in the conformational isomer **2′** depicted in the right-hand side of Scheme 4. Transformation of **2** to **2′** involves rotation about one of the Pd−P bonds and concomitant displacement of the central benzene ring of **1** in relationship to the $PdCl_2P_2$ plane. Such a movement of the central benzene ring might account for the complexity of the aromatic signals shown in Figure 4. In addition, this isomer would be expected to have a dipole moment different from that of **2** and thus could rationalize the solvent dependency

Scheme 5. Preparation of 4

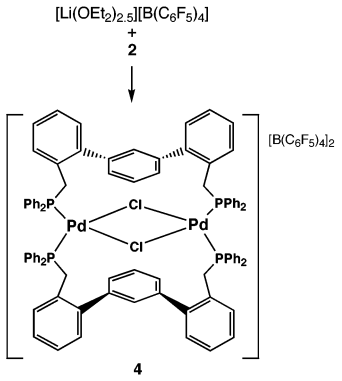

of the fluxional behavior. The energy difference between **2** and **2′** is estimated to be only 1.4 kcal/mol by these calculations (calculations for **2** were performed by constraining ligand geometry and for **2′** by using no constraints). Such a small energy difference could easily be modulated by either solvent effects or crystal-packing forces. As the two isomers do not significantly change the phosphorus environments, only a single averaged signal would be expected (and is seen). Due to the incomplete resolution of all of the signals involved, the limited solubility of **2** in $CDCl_3$ and C_6D_6, and the corresponding lack of good ^{13}C NMR data, a more complete picture of the solution dynamics of **2** is unavailable at this time.

In the course of studies to explain the dynamic behavior of **2**, the possibility that dissociation of one of the chloride ligands and formal η^2 binding of the central benzene was examined. These efforts led to the isolation of **4** (below) and helped rule out halide dissociation as being responsible for the variable-temperature NMR behavior of **2**.

On the basis of the proximity of H(1) to the metal centers in **2** and **3** (M−H(1) = ca. 3.5 Å), and the reactivity of other pincer metal−phosphine complexes, it was anticipated that insertion of the metal center into the C(1)−H(1) bond might be induced. Many pincer-type ligands often undergo insertion under relatively mild conditions, such as refluxing solutions of the ligand with metal salts in solution. Compound **2** was thus subjected to similar conditions. However, no new species were observed in the ^{31}P NMR spectrum after heating to 100 °C in either dichloromethane or benzene in a sealed vessel for 48 h, or even after heating to 140 °C in DMF under N_2 for 24 h. Since the desired insertion process would necessitate elimination of HCl, the aforementioned reactions were repeated in the presence of excess triethylamine as a base to help promote the reaction. However, the same results were obtained as in the base-free trials. Thermolysis of solid-state samples has also been reported to lead to intramolecular C−H bond insertion by metal phosphine complexes.[14] However, progressive heating of solid **2** under nitrogen or in vacuo did not appear to produce the desired species either. Monitoring such thermolysis reactions by ^{31}P NMR spectroscopy revealed only **2** up to the decomposition point of the compound to an intractable black tar at around 300 °C.

(14) Baltensperger, U.; Gunter, J. R.; Kagi, S.; Kahr, G.; Marty, W. *Organometallics* **1983**, *2*, 571−578.

Chart 1

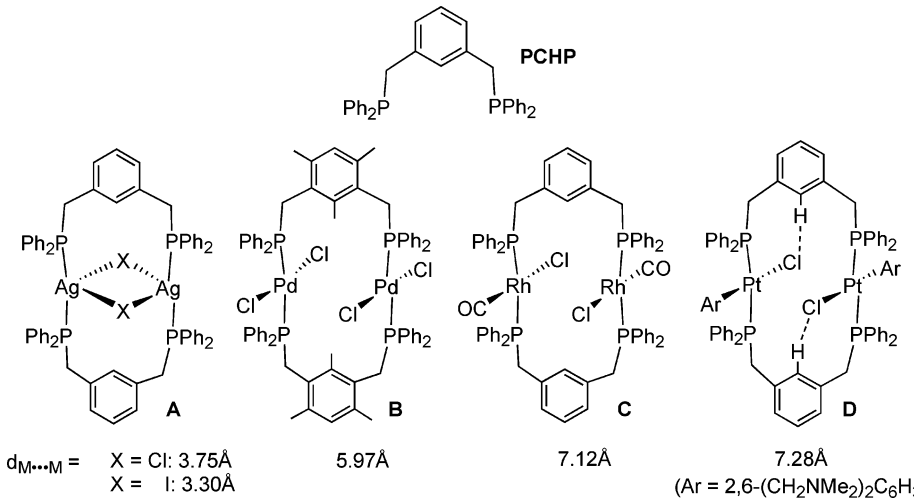

Table 3. Select Bond Lengths (Å) and Angles (deg) for 4

Pd(1)−P(1)	2.2576(26)	Pd(1)−Cl	2.4057(24)
Pd(1)−P(2)	2.2785(26)	Pd(1)−Cl(A)	2.4142(25)
P(1)−Pd(1)−P(2)	97.04(10)	Pd(1)−Cl−Pd(1A)	96.26(9)
P(2)−Pd(1)−Cl	91.56(9)	P(1)−Pd(1)−Cl	165.67(10)
P(1)−Pd(1)−Cl(A)	90.24(9)	P(2)−Pd(1)−Cl(A)	166.51(10)
Cl−Pd(1)−Cl(A)	83.74(8)		

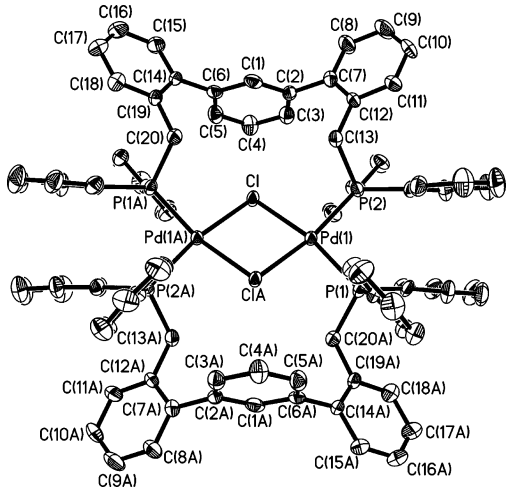

Figure 6. ORTEP drawing of the molecular structure of **4**. Hydrogen atoms and $[B(C_6F_5)_4]^-$ anions are omitted for clarity.

As an alternative route to such a product, attempts were made to obtain a Pd^0 complex by reaction of **1** with $Pd_2(dba)_3$. These reactions produced multiple products, and Pd metal was observed in the reaction vessels. Reduction of **2** by heating of a DMF solution in the presence of Zn metal did produce a single soluble species, as ascertained by ^{31}P NMR spectroscopy (δ 27.8), but only in low yields and in conjunction with Pd black.

As another strategy undertaken to enhance the reactivity of **2**, and as a means to address the possibility of halide dissociation as an explanation for the complicated ^1H NMR spectra of **2**, the reaction of $[Li(OEt_2)_{2.5}][B(C_6F_5)_4]$ with **2** was examined. Reaction of **2** with 1 equiv of $[Li(OEt_2)_{2.5}][B(C_6F_5)_4]$ in dichloromethane affords a new species (**4**) that is characterized by a single ^{31}P NMR resonance at δ 46.3 (Scheme 5). Unlike **2** and **3**, **4** displays sharp ^1H NMR resonances and is consistent with its formulation as $[(\mathbf{1})PdCl][B(C_6F_5)_4]$. Compound **4** is also properly analyzed for this formula. However, X-ray analysis of a crystal grown by diffusion of *n*-pentane into a dichloromethane solution of **4** revealed an unexpected rearrangement of phosphine binding sites. The actual structure consists of a chlorine-bridged dipalladium core in which each Pd center is coordinated to *one* of the phosphine binding sites from *each* diphosphine **1** (Table 3 and Figure 6). A Pd···Pd distance of 3.60Å is realized in this structure.

Although this type of cross-core bridging is fairly common for some other M_2Cl_2 cores (i.e., common "A-frame" ligands such as a recently reported and structurally characterized Rh_2Cl_2-core bridging diphosphine),[15] structurally characterized compounds are rarer for palladium. Other structurally characterized examples of bridging across a single Pd_2Cl_2 core have been reported that do not feature a diphosphine as the bridging moiety.[16] In contrast to **4**, the previous examples featured long and highly flexible linking groups. Comparisons to the commonly employed "PCHP" pincer type ligands (Chart 1, top) are natural. This particular ligand, in its nonmetalated form, and its disilver complexes offer M···M distances comparable to those seen in **4**.[17a] Some other examples shown in Chart 1 illustrate longer M···M distances.[17b−d]

Interestingly, the orientation of the Pd_2Cl_2 core in **4** directs the chlorine atoms toward the face of the central benzene ring of **1**, but at a distance (3.66 Å) greater than that observed in **2** (3.33 Å). Finally, the benzyl protons in **4** are found to resonate as two sets of multiplets at δ 4.10 and 4.79. The latter signals are again ascribed to those being vicinal to the chloride ligands (ca. 2.60 Å in the X-ray structure of **4**). These short intramolecular

(15) Ini, S.; Oliver, A. G.; Tilley, T. D.; Bergman, R. G. *Organometallics* **2001**, *20*, 3839−3841.

(16) (a) Hambley, T. W.; Raguse, B.; Ridley, D. D. *Aust. J. Chem.* **1985**, *38*, 1455−1460. (b) Kleij, A. W.; Gebbink, R. J. M. K.; van den Nieuwenhuijzen, P. A. J.; Kooijman, H.; Lutz, M.; Spek, A. L.; van Koten, G. *Organometallics* **2001**, *20*, 634−647.

(17) (a) Caruso, F.; Camalli, M.; Rimml, H.; Venanzi, L. M. *Inorg. Chem.* **1995**, *34*, 673−679. (b) van der Boom, M. E.; Gozin, M.; Ben-David, Y.; Shimon, L. J. W.; Frolow, F.; Kraatz, H.-B.; Milstein, D. *Inorg. Chem.* **1996**, *35*, 7068−7073. (c) Dilworth, J. R.; Zheng, Y.; Griffiths, D. V. *J. Chem. Soc., Dalton Trans.* **1999**, 1877−1881. (d) Albrecht, M.; Dani, P.; Lutz, M.; Spek, A. L.; van Koten, G. *J. Am. Chem. Soc.* **2000**, *122*, 11822−11833.

Scheme 6. Calculated Structures for the Conversion of 2 to 5

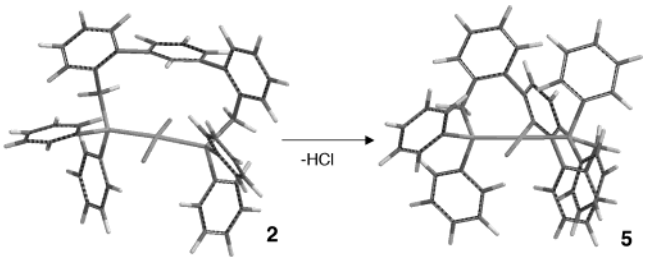

CH···Cl contacts are very reminiscent of the weak hydrogen bonding noted for **D** (Chart 1, $d_{CH\cdots Cl} = 2.66$ Å).[17d]

It is interesting to now examine the factors that might prevent the metalation of the vicinal C−H bond of **1**. The putative pincer binding mode of **1** at a palladium center was modeled using SPARTAN (PM3). Analysis of the resulting structure showed no evidence for unusual bond lengths or angles about the metal center (**5**; Scheme 6). This calculation, in conjunction with that for **2** (above), allows an estimate of −1.3 kcal/mol for ΔH_{rxn} for the transformation of **2** to **5**. In addition to the marginal enthalpy of reaction for the insertion process, the nature of the chelate structure may place some constraints that result in a prohibitively high reaction barrier. For example, **2** may not allow a sufficiently close Pd···H distance required for insertion. Alternatively, it may be that the key step requires a close CH···Cl interaction for the resulting incipient release of HCl (and concomitant attack on metal center on the arene).[17d] If true, then **2** with its long C(1)−H(1)···Cl(1) distance of 4.51 Å could be limiting the activation of the C(1)−H(1) bond. Either way, it appears that the successful synthesis of complexes bearing this type of *m*-terphenyl-based ligand in a true "pincer" binding mode may require the premetalation approach.[9]

In conclusion, a representative diphosphine based on a *m*-terphenyl scaffold has been prepared. Diphosphine complexes of $NiCl_2$ and $PdCl_2$ display a good degree of thermal stability and have thus far not been observed to undergo C−H bond insertion analogous to that observed in simple pincer complexes. X-ray structural analyses of neutral Ni and Pd complexes indicate that the diphosphine binds in a trans geometry with a bite angle near 180°. X-ray analysis of a dicationic Pd complex revealed a dimeric structure in which the diphosphine is engaged in an unusual cross-core bridging mode. Investigations featuring other donor functionalities built upon this framework are underway to explore the reactivity and possible pincer binding modes of this motif.

Acknowledgment. We thank the National Science Foundation (Grant No. CHE-0202040) for support and Dr. Philip Mountford (Oxford University) for enlightening discussions.

Supporting Information Available: X-ray crystallographic files in CIF format for the structures of **2**−**4**. This material is available free of charge via the Internet at http://pubs.acs.org.

OM049662D